

LITHIUM IN EARLY F DWARFS

ANN MERCHANT BOESGAARD¹ AND MICHAEL J. TRIPICCO¹

University of Hawaii, Institute for Astronomy
 Received 1985 June 25; accepted 1985 October 9

ABSTRACT

Abundances have been determined for Li in early F field dwarfs in order to determine the initial Li content for Population I stars and to examine the degree and nature of the depletion of Li in stars in this mass range during their early evolution. With high resolution, high signal-to-noise (S/N) spectra from the Canada-France-Hawaii telescope and Reticon detector at the coudé spectrograph it has been possible to make observations of weak features ($W_\lambda \leq 2$ mÅ) and so to push the observations to hotter temperature stars and to greater levels of Li depletion. Reticon spectra were obtained of 75 F0–F5 dwarfs with a spectral resolution of 0.11 Å and S/N values in the continuum of ~ 400 –600. Model atmospheres of Kurucz were used to calculate abundances from the Li I and Li I–Fe I blends, five Fe I lines, and one Ca I line.

Lithium at the initial or “cosmic” abundance level was present in about one-third of the stars observed; the mean value is $\text{Li}/\text{H} = 1.02 \times 10^{-9}$ or $\log N(\text{Li}) = 3.01$. The stars with this abundance are preferentially the hottest ($T > 6500$ K) and the youngest (age $< 2 \times 10^9$ yr) stars in the sample. Seventeen percent show Li depletions from this initial value by factors of 3–10, and 53% are further depleted by factors of 10–150. Lithium content and age are related with 62% of the stars younger than two billion years being Li-rich and 64% of the stars older than that being depleted by more than factors of 40. The oldest stars on kinematic grounds all have severe Li depletions. A large range in Li abundance at each age shows that other parameters influence the Li depletion.

For the Li-rich stars the $[\text{Fe}/\text{H}]$ abundances are all within a factor of 2 of the solar abundance; there is a greater range in metallicity for stars with low Li upper limits [$\log N(\text{Li}) \leq 1.0$]. For $[\text{Fe}/\text{H}]$ between -0.2 and $+0.2$ there is a uniform distribution in $\log N(\text{Li})$ from < 0.9 to $+3.2$. Chromospheric activity, as measured by Ca II HK emission fluxes is low in early F stars (relative to G dwarfs) and a hint of a trend—where enhanced activity and higher Li go together—may be present. High rotation with high Li and slow rotation with low Li seem to be the normal combinations, but there are some interesting exceptions to this pattern; these “misfits” are Hyades-like in their rotation, metallicities and low Li abundances in the temperature region ~ 6400 K.

Subject headings: stars: abundances — stars: chromospheres — stars: rotation

1. INTRODUCTION

The maximum value for Li/H in Population I objects is uniformly found to be 10^{-9} for meteorites, young T Tau stars, F and G dwarfs in galactic clusters and in the field (see Boesgaard 1976 and Duncan 1981 for summaries). Furthermore, standard stellar model calculations indicate that the surface convection zones in early F dwarfs are too shallow to deplete surface Li, and indeed past observations of Li in F stars in open clusters showed little or no evidence for depletion. Therefore one would expect that early F stars in the field also would have the “initial” $\text{Li}/\text{H} = 10^{-9}$. Observations by Danziger and Conti (1966) and the summary by Herbig and Wolff (1966) had already shown that this was not the case; slightly more than half of the 22 F0–F4 dwarfs had no detectable Li feature.

Theoretical calculations by Bodenheimer (1965) of Li depletion by convective mixing to high enough temperatures for (p, α) reactions to occur during pre-main-sequence evolution predict that early F dwarfs with $B-V < 0.4$ should arrive on the main sequence with their original surface Li/H abundance unaffected. His assessment of the uncertainties in the calcu-

lations (e.g., in the assumed value of l/H , the mixing length to the scale height) was that the depletion pattern could move to lower $B-V$ values by 0.05. Even so, it was expected that stars with $B-V$ of 0.4–0.45 would not be depleted by more than 5%–10% in Li/H . There is a short discussion of Li depletion in a paper by Mazzitelli and Moretti (1980) on pre-main-sequence D burning in which they report greater pre-main-sequence Li depletion in the Sun than Bodenheimer found, in part because they use $l/H = 2.0$. However, as shown by Duncan and Jones (1983) and by Cayrel *et al.* (1984), neither Pleiades nor Hyades dwarfs near the solar temperature show significant depletion: none for the Pleiades and 5% of the solar depletion for the Hyades. Therefore, theoretical expectation makes it seem unlikely that the solar depletion occurs during the pre-main-sequence phase. Furthermore, only about half of the field stars near the solar effective temperature (T_e) show depletions of 50% or more (Duncan 1981) which also argues against a significant pre-main-sequence depletion source.

Recently, calculations of Li depletion in both pre-main-sequence and main-sequence stars with masses from 0.7 to $1.2 M_\odot$ have been done by D’Antona and Mazzitelli (1984) for various values of Y , Z , l/H , and amounts of ad hoc “extra mixing.” They conclude that some such extra mixing below the convection zone is necessary to explain the observed Li deple-

¹ Visiting Astronomer at the Canada-France-Hawaii Telescope, operated by the National Research Council of Canada, the Centre National de la Recherche Scientifique of France, and the University of Hawaii.

TABLE 1
SPECTROSCOPIC OBSERVATIONS

HR	Name	HD	Sp	Night ^a	S/N	Remarks	HR	Name	HD	Sp	Night ^a	S/N	Remarks
3579	...	76943	F5 V	2	550	Spectroscopic binary	6467	...	157373	F4 V	2	480	
3857	13 LMi	83951	F3 V	2	440		6489	...	157856	F3 V	2	480	
3954	...	87141	F5 V	3	480		6541	...	159332	F6 V	1,2	630	δ Set variable?
3979	...	87822	F4 V	3	490		6569	λ Ara	160032	F3 IV	3	460	
4090	30 LMi	90277	F0 V	1	630	Two observations	6594	...	160910	F4 V	1,2	630	
4150	35 LMi	91752	F3 V	2	460		6595	58 Oph	160915	F6 V	4	460	
4230	44 LMi	93765	F3 V	3	480	Spectroscopic binary	6596	ω Dra	160922	F5 V	2	450	Spectroscopic binary, Hyades group
4408	81 Leo	99285	F2 V	2	440		6600	...	161023	F0 V	3	480	
4421	...	99747	F5 V	3	500		6670	...	162917	F3-5 IV-V	3	440	
4431	58 UMa	99984	F4 V	2	440		6734	τ Oph	164765	F2 V	4	440	
4455	89 Leo	100563	F5 V	2	450		6797	...	166285	F5 V	1,2	630	
4501	62 UMa	101606	F4 V	1,2	680		6844	...	167858	F2 V	2	430	
4600	...	104731	F6 V	3	430		6850	36 Dra	168151	F5 V	1	370	
4657	...	106516	F5 V	3	480		6985	...	171802	F5 V	1,2,3	430, 450, 420	Spectroscopic binary
4803	...	109799	F1 IV	3	510	UMa stream	7000	...	172103	F1 IV-V	3	440	Spectroscopic binary
4825	γ Vir S	110379	F0 V	1	485		7163	...	176095	F5 IV	3	440	
4826	γ Vir N	110380	F0 V	1	670	Two observations	7247	...	178089	F2 V	3	410	
4914	α ¹ CVn	112412	F0 V	2	450		7322	...	181096	F6 V	2	380	
4926	...	113022	F6 Vs	2	390	Hyades moving group	7354	...	182101	F6 V	3	450	
4934	...	113337	F6 V	1	430		7496	...	186185	F5 IV	3	450	
4946	39 Com	113848	F4 V	3	370		7697	...	191195	F5 V	3	490	
5074	...	117200	F0	4	470	Common proper motion	7727	68 Dra	192455	F5 V	3	440	
5075	...	117201	F0	4	490	Common proper motion	7756	...	192985	F5 V:	2	470	
5110	...	118216	F2 IV	3	450	Spectroscopic binary RS CVn	7925	...	197373	F6 IV	3	430	
5156	...	119288	F3 Vp	1	430		7936	ψ Cap	197692	F4 V	4	400	
5347	...	125111	F2 IV	2	390		7973	15 Del	198390	F5 V	1	440	
5387	...	126141	F5 V	3	440		8205	...	204121	F5 V	2	475	
5445	...	128093	F5 V	2	400		8222	...	204577	F0 V	3	390	
5455	...	128429	F5 V	3	480		8354	15 Peg	207978	F4 V	1	450	
5529	...	130817	F2 V	1,2	590		8400	16 Cep	209369	F5 V	3	470	
5533	38 Boo	130945	F5 V	1	440		8507	...	211575	F3 V	2	480	
5758	...	138290	F4 V	3	510		8514	...	211976	F6 V	2	430	
6052	...	145976	F3 V	2	480		8805	5 And	218470	F5 V	3	500	
6181	...	150012	F5 IV	3	460		8825	6 And	218804	F5 IV	3	470	
6189	...	150177	F3 V	3	440		8885	12 And	220117	F5 V	3	430	
6193	...	150366	F0 V	3	415		8907	o Gru	220729	F4 V	5	230	
6290	...	152830	F3 Vs	4	440	δ Set variable	8977	...	222451	F1 V	3	430	Hyades group
6445	ξ Oph	156897	F1 V	1	450								

^a Night 1—UT 1983 May 3; night 2—UT 1984 Jun 10; night 3—UT 1984 Jun 11; night 4—UT 1984 Jul 6; and night 5—UT 1984 Dec 11.

tions; to achieve adequate Li destruction without destroying Be, they find that the extra mixing should occur during pre-main-sequence evolution. For $1.2 M_{\odot}$, corresponding to F5–F6, with extra mixing they can achieve depletions of 0.613, or to Li/H of 6.1×10^{-10} ; even this rather small amount of depletion becomes even less for higher mass (earlier spectral type) stars.

Extension of mixing by turbulent diffusion on the main sequence has been discussed by Baglin, Morel, and Schatzman (1985). They find a good match of the theory with the Hyades observations of the lower main-sequence stars of Cayrel *et al.* (1984) if the turbulence is generated by a temperature imbalance due to rotation and the resulting meridional circulation and differential rotation. The expected amount of depletion is inversely proportional to mass, so no depletion would be expected in the F stars.

Perhaps a more important way to achieve mixing in the F stars is by gravitational settling of Li atoms below the convection zone as described by Vauclair *et al.* (1978). Another possibility is through convective overshoot, which Strauss, Blake, and Schramm (1976) show is favored by the energetics available in the higher mass stars although the convective zone is shallower and the temperature difference to be spanned to destroy Li is larger than in the G stars.

Early observations in the Hyades F stars by Wallerstein, Herbig, and Conti (1965) reveal six middle-F stars with no detectable Li line, four of which have upper limits about 2–3 times less than stars with both smaller and larger $B - V$ values. The observations of Zappala (1972) of Li in open clusters (Pleiades, Hyades, Praesepe) indicate little if any Li depletion in the 10 F dwarfs, although two rather high upper limits to Li/H make this uncertain. Our own observations in the Hyades F dwarfs concurrent with this work show that very large Li depletions are present in the middle F stars, with “cosmic” Li abundances on either side in the early and late F dwarfs.

In the high-temperature F stars Li is very highly ionized ($\text{Li I}/\text{Li} \approx 10^{-3}$) and the Li I resonance line very weak; for example, at 7500 K the predicted equivalent width for $\text{Li}/\text{H} = 10^{-9}$ is 20 mÅ, or at the solar abundance of 10^{-11} it is 0.2 mÅ. The solar abundance would give a 1 mÅ line at 6500 K. With the aid of high resolution, high signal-to-noise observations with modern detectors it is possible to examine the distribution of Li abundances (based on the weak Li I line) in early F stars. As a group these stars must be young (compared to the solar lifetime) to still be on the main sequence. Both because of their relative youth (total main-sequence lifetimes are about $2\text{--}4 \times 10^9$ yr) and because no Li depletion is expected by theory, the observed maximum Li/H values should reveal the initial abundance for this type of star unambiguously. This will provide a more accurate benchmark for initial Li in Population I galactic disk stars for comparison with that found for Population II halo stars by Spite, Maillard, and Spite (1984). The early work on early F stars was done photographically (Herbig 1965; Danziger and Conti 1966; Feast 1966; Zappala 1972). We discuss here high signal-to-noise Reticon observations made with the Canada-France-Hawaii coude spectrograph of 75 F0–F5 dwarfs. The greater accuracy of the Reticon detector over photographic plates enables us to investigate the extent of the depletion in this spectral range and to explore the character of the depletion via its relationship to other parameters such as metallicity, rotation, chromospheric activity, and evolutionary age.

II. OBSERVATIONS

The observations were made with the coude spectrograph of the Canada-France-Hawaii 3.6 m telescope and the f/7.4 camera and an 830 lines mm^{-1} mosaic grating blazed in the first-order red at 8040 Å. The detector used was a liquid nitrogen cooled, integrating 1872 photodiode Reticon array (Walker, Johnson, and Yang 1985). This system provides a spectral coverage of ~ 135 Å centered at ~ 6700 Å near the Li I line with a resolution of 0.112 Å and a reciprocal dispersion of 4.83 Å mm^{-1} or $0.0723 \text{ Å pixel}^{-1}$. Spectra were obtained of 75 F0–F5 dwarfs on five nights: 1983 May 3, 1984 June 10 and 11, 1984 July 6, and 1984 December 11 UT. Spectra of six of the stars were taken on two different nights, and since no systematic differences were found, these were co-added. All of the stars were exposed to high signal-to-noise ratio levels with the value in the continuum typically 400–600. Table 1 lists the stars observed with their spectral types, the night of the observation and the approximate signal-to-noise ratio level in the continuum.

Multiple collections of four flat-field exposures were taken each night at levels representative of the mean exposure for various subsets of the program stars for that night. The instrumental response was removed by averaging the appropriate four flat-field exposures and dividing the stellar spectrum by the flat field. Any minor nonlinearities which may have remained were then corrected by applying a four-channel normalization procedure which equalizes the total output from the four channels. The Li I region in a sample of reduced spectra is shown in Figure 1.

Equivalent widths (W_{λ}) were measured for the Li I resonance line at $\lambda 6707$, for the Ca I line at $\lambda 6717$, and for five Fe I lines in the vicinity. At these wavelengths continuum placement is straightforward, and the high signal-to-noise ratio and high spectral resolution of the data allowed lines to be detected with equivalent widths as low as 1 mÅ. In cases of marginal detection or nondetection of the Li I line, an upper limit to W_{λ} was obtained by summing over the appropriate spectral interval. Table 2 contains the W_{λ} measurements of the measurable Li I, Ca I, and five Fe I lines in the 75 stars. In the cases of the double-lined spectroscopic binaries the measurements are given for both components from the technique described in § IIIa, below.

III. ANALYSIS

a) Temperatures

Effective temperatures for nearly all the stars in the sample were determined from published Strömgren β photometry. The (β , θ_e) relation of Hearnshaw (1974) yields temperatures ($T_e = 5040/\theta_e$) calibrated to Johnson's (1966) scale from his ($R - I$) index. Five of the program stars did not have published β values, but ($R - I$) colors were available and so temperatures for these stars (HR 4090, 4803, 4825, 4914, and 6193) could be placed on the same scale. In only two cases (HR 6052 and 7247) were neither β nor ($R - I$) values available; for these stars published Strömgren ($b - y$) colors and the ($[b - y]$, T_e) relation of Oblack and Charetan (1980) were used to determine effective temperatures. Oblack's temperature scale was found to differ from the Hearnshaw/Johnson one by only a small zero-point shift (~ 100 K), and the resultant temperatures were thus placed on the same T_e scale as the rest of the sample. The relevant photometry and the resultant T_e 's are given in Table 3.

Six of the stars in the sample (HR 3579, 4230, 5110, 6596,

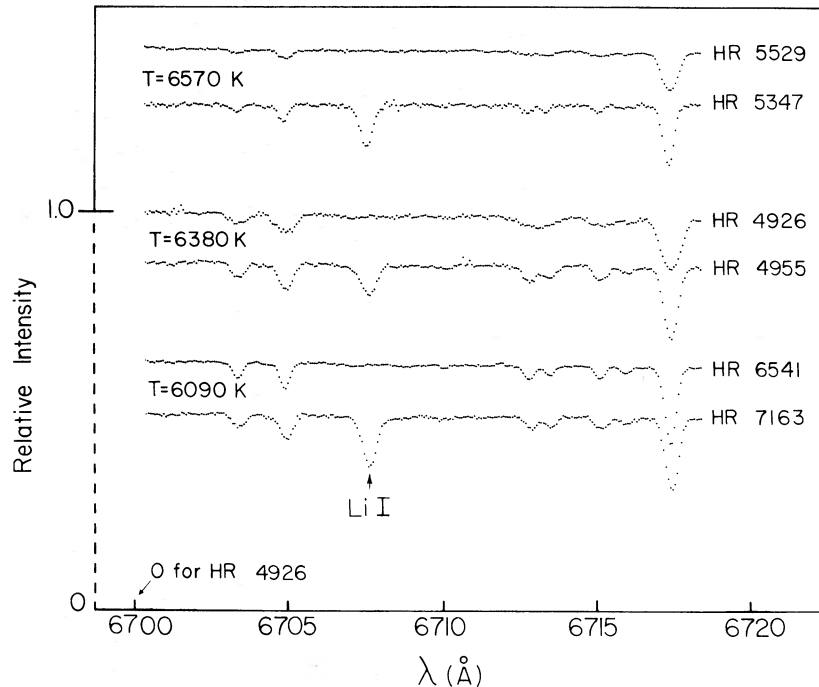


FIG. 1.—Sample spectra of three “matched pairs” of F stars. The pairs have similar temperatures, metallicities, $v \sin i$ values, but very different Li I line strengths. The vertical scale is the same for all six spectra, but only indicated for HR 4926. The strong line on the right is Ca I λ 6717; the two shortward of Li I are Fe I λ 6703 and λ 6705.

6985, and 7000) were found to be double-lined spectroscopic binaries. A sample spectrum in the Li I region of HR 6985 is shown in Figure 2; the spectra of the two components are very similar except for the presence of strong Li λ 6707 in one and its absence in the other. Temperatures determined from photometric quantities are clearly inappropriate for these systems, and so a method was devised by which estimates of T_e for each component in each of the binaries could be made. The ratio of the equivalent widths of the two Fe I absorption lines at 6703 Å and 6705 Å was found to vary linearly with temperature in

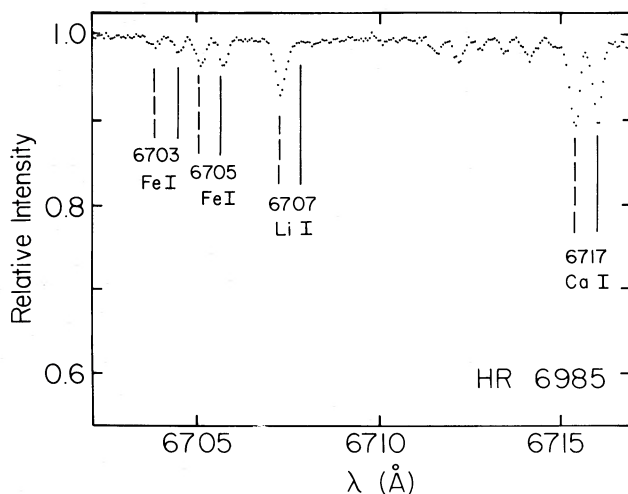


FIG. 2.—Spectrum of the double-lined spectroscopic binary HR 6985. Some spectral features in one of the stars are indicated by the dashed lines and in the companion by the solid lines. Although the strengths of most spectral features are the same—indicating similar temperatures for the two components—the Li I line is strong in one and absent in the other.

the stars for which T_e 's were determined as described above. This empirical relationship is presumably due to the difference in the lower excitation potentials of the two lines: 2.75 and 4.59 eV, respectively. Points for the Sun and Arcturus were also included in defining this relation in order to extend it to cooler temperatures; they were found to lie very close to the fit calculated for the early F stars alone. The relation is shown in Figure 3, and the fit is given by the formula

$$W(6703)/W(6705) = 2.723 - 3.446(10^{-4})T_e. \quad (1)$$

The measurement of this equivalent width ratio for the lines of each component in a particular binary yields T_e . This procedure was employed except for HR 3579 where the spectral types were thought to be better indicators of the temperatures. Once the temperature of each component is known, the measured equivalent widths can be scaled to reflect the unequal contribution of each component to the total continuum flux. The ratio of the Planck functions at 6700 Å is given by

$$\frac{B_\nu(b)}{B_\nu(r)} = \frac{e^{2.146 \times 10^4/T_r} - 1}{e^{2.146 \times 10^4/T_b} - 1},$$

where b and r refer to the component whose lines were blueward (b) and redward (r) at the time of our observation. The multiplication factors are then

$$mf(b) = 1 + \left[\frac{B_\nu(r)}{B_\nu(b)} \times \frac{R^2(r)}{R^2(b)} \right]$$

and

$$mf(r) = 1 + \left(\frac{B_\nu(b)}{B_\nu(r)} \times \frac{R^2(b)}{R^2(r)} \right)$$

This information is contained in Table 4.

In all but two systems the two components were found to

TABLE 2
EQUIVALENT WIDTHS (mÅ)

HR	Fe I 6677.993 Å	Fe I 6703.573 Å	Fe I 6705.117 Å	Fe I + Li I 6707.441 Å, 6707.761 Å, 6707.912 Å	Ca I 6717.685 Å	Fe I 6726.668 Å	Fe I 6750.152 Å
3579 ^a/...	3/20	8/34	≤4/14	15/...	12/34	34:/44
3857....	98.0	14.3	28.6	8.2	89.5	25.4	41.1
3954....	116.3	21.2	34.7	17.0	108.1	37.0	58.6
3979....	105.3	19.6	42.1	44.6	103.9	34.4	50.1
4090....	98.7	6.2	19.8	...	77.7	21.4	27.2:
4150....	90.8	12.1	21.5	...	83.6	22.6	41.7
4230....	77/85	7/6	18/15	11/2	66/90	16/13	34/23
4408....	88.8	7.4	16.6	63.8	83.8	22.0	25.6
4421....	68.1	4.9	11.4	≤2.3	54.1	11.9	20.9
4431....	97.8	14.6	21.6	54.7	83.8	24.1	47.8
4455....	108.6	22.4	40.9	51.6	107.7	35.9	51.7
4501....	60.2	5.9	9.7	≤2.3	56.4	9.3	21:
4600....	90.3	11.0	22.4	≤3.5	81.3	24.2	35.0
4657....	70.4	6.0	12.1	≤6.3	63.1	12.8	23.7
4803....	95.5	56.0	83.9	22.4	22:
4825....	108.3	10.2	16.9	50.5	61.2	19.2	22.2
4826....	93.6	9.4	20.2	56.1	66.7	21.2	23.3
4914....	84.2	7.3	17.7	39.5	73.9	20.9	24.2
4926....	112.5	18.8	35.9	≤7.1	110.3	39.3	52.8
4934....	103.4	15.5	31.8	≤5.1	96.5	31.7	45.3
4946....	81.4	10.0	19.6	67.5	74.1	≤18.9	33.7
5074....	98.9	12.6	26.8	74.9	89.3	25.2	33.3
5075....	98.6	13.1	27.2	≤2.5	92.7	25.6	38.0
5110 ^a ...	24/83	13/9	10/18	21 ^b /...	21/64	10/17	16/20
5156....	93.4	10.2	24.1	≤2.4	77.1	18.8	33.6
5347....	84.3	11.0	19.3	54.7	68.8	20.1	30.2
5387....	91.1	10.8	24.8	≤5.2	84.3	27.6	38.1
5445....	99.2	14.2	29.2	≤4.6	87.3	26.2	43.2
5455....	100.2	15.6	26.8	≤6.2	94.7	28.6	45.7
5529....	76.0	4.3	12.3	≤1.0	68.7	14.9	27.6
5533....	117.4	17.7	35.9	9.6	100.3	31.2	47.8
5758....	93.1	10.0	22.7	47.2	75.0	19.1	33.1
6052....	90.5	8.6	25.5	32.2	81.6	20.3	28.2
6181....	118.6	16.7	38.0	34.2	108.2	31.8	46.2
6189....	78.5	10.0	12.9	38.2	64.8	14.8	32.4
6193....	55.3	27.9	57.6	11.5	...
6290....	97.0	5.9	15.7	32.7	91.0	18.0	25.8
6445....	86.0	7.9	18.5	≤5.4	66.4	16.8	29.7
6467....	77.6	8.2	16.7	≤3.3	61.4	14.3	27.6
6489....	98.9	14.9	29.9	92.9	88.1	23.5	44.7
6541....	97.6	16.9	27.3	≤6.2	94.2	29.0	50.8
6569....	86.9	8.8	19.6	≤2.6	74.9	21.9	29.4
6594....	95.5	7.5	16.3	22.8	90.0	17.9	39.8
6595....	96.8	14.3	28.0	28.8	86.1	26.9	43.3
6596....	145/78	17/9:	42:/24	116/64	138/69:	42/22	72/37
6600....	79.6	7.5	18.9	≤2.6	70.1	18.1	27.3
6670....	107.1	21.3	40.9	≤4.0	95.7	32.1	46.5
6734....	114.0	14:	30:	81.2	104.0	28.7	48.1
6797....	97.2	13.4	26.5	≤5.6	92.8	30.9	46.6
6844....	88.2	13.4	27.1	36.5	78.6	18.3	26.7
6850....	89.9	9.9	18.0	≤4.0	66.8	19.9	32.4
6985....	94/101	10/17	26/32	58/≤8	84/94	21/33	35/47
7000....	81/...	5/2	22/22	72/96	80/...	26/25	71:/...
7163....	106.3	17.2	32.6	73.9	102.8	30.9	51.3
7247....	89.9	14.5	26.1	75.9	85.7	22.1	33.3
7322....	91.4	15.5	25.2	≤3.5	85.0	22.0	41.9
7354....	96.2	14.4	30.3	6.5	89.6	25.7	42.4
7496....	116.1	17.3	36.7	≤5.1	108.8	35.8	53.0
7697....	103.8	15.2	32.1	...	99.4	31.5	47.6
7727....	115.6	23.6	43.0	≤7.6	115.2	36.4	57.1
7756....	101.8	14.0	30.5	≤4.2	89.8	28.8	48.0
7925....	103.7	15.7	31.3	≤2.3	98.7	32.2	46.3
7936....	110.3	12:	32:	≤3.8	87.6	35.6	42:
7973....	105.4	11.8	20.8	20.3	65.7	19.8	42.6
8205....	109.5	21.2	34.2	22.8	111.7	32.7	50.4
8222....	109.3	14.0	24.4	56.1	94.6	23.8	38.7
8354....	80.9	7.3	11.9	7.9	55.5	12.9	24.0
8400....	103.3	15.0	25.5	19.4	88.6	24.0	44.2
8507....	110.6	18.5	41.5	≤2.8	101.8	33.7	47.5

TABLE 2—Continued

HR	Fe I 6677.993 Å	Fe I 6703.573 Å	Fe I 6705.117 Å	Fe I + Li I 6707.441 Å, 6707.761 Å, 6707.912 Å	Ca I 6717.685 Å	Fe I 6726.668 Å	Fe I 6750.152 Å
8514....	96.9	13.2	22.4	23.4	95.4	26.6	45.6
8805....	92.3	13.1	22.9	≤3.0	87.7	24.8	41.5
8825....	93.1	14.8	25.7	≤2.3	89.0	23.4	41.0
8885....	108.0	18.1	30.5	5.3	103.8	33.2	51.4
8907....	70.0	10.2	20.4	63.8	77.6	21.0	32.0
8977....	110.0	15.5	35.1	≤4.2	101.7	29.9	44.0

^a The equivalent widths listed are those actually measured, not those multiplied by the factors in Table 4 for HR 3579 and HR 5110 because the temperatures of the components are different from each other and are uncertain.

^b Likely to be Fe I 6707.4 only.

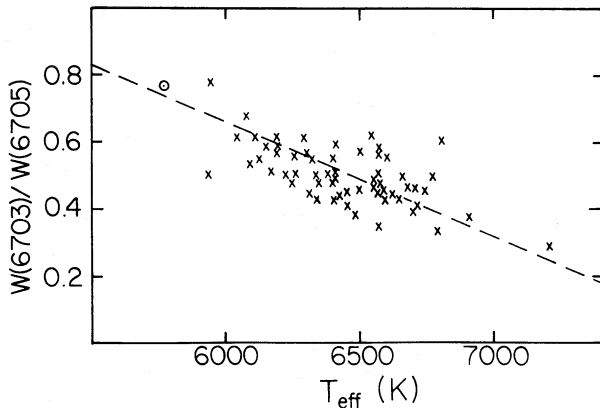


FIG. 3.—The measured equivalent width ratio of two Fe I features of different excitation potential plotted as a function of temperature derived from $H\beta$ for the stars in our sample. The Sun is the circled dot. The dashed line represents the relationship used to estimate the temperatures for each component of the double-lined spectroscopic binaries where the two features could be measured. Because the $H\beta$ photometry was for the combined light, it could not be used to estimate the individual temperatures.

have temperatures within 400 K of each other. One exception is HR 5110, a well-known RS CVn binary which Conti (1967) concluded consists of an early F primary and a G–K secondary. Spectra of both components are clearly visible; the temperatures we have determined by means of our empirical relations are consistent with this picture of the system (see Table 3).

b) Gravities, Microturbulence, Magnitudes, and Ages

The surface gravity, absolute visual magnitude, and age for each of the stars were determined from published Stromgren photometric indices. The F-star standard relations for $c_1(\beta)$ and $M_v(\text{ZAMS}, \beta)$ were taken from Crawford (1975). For each star $\delta c_1 \equiv c_1(\text{obs}) - c_1(\text{standard})$ was formed and Crawford's absolute magnitude calibration $M_v = M_v(\text{ZAMS}, \beta) - (9 + 20\Delta\beta)\delta c_1$ (where $\Delta\beta = 2.720 - \beta$) was used to calculate M_v and ΔM_v . Following Duncan (1984) we let $\log g$ (ZAMS) = 4.3 and the surface gravity for each star was determined via $\Delta \log g = \Delta M_v/2.5$. Ages were then obtained from isochrones with $X = 0.70$, $Z = 0.03$ from Maeder (1976). Any star having $\delta c_1 \leq 0.03$ lies too close to the ZAMS for a reliable age to be determined. In order for this analysis to be done for the few stars without published β values, their temperatures

(having been calculated as described in § IIIa above) were converted into pseudo- β values via the Hearnshaw (β, θ_e) relation. All these results are given in Table 3. Also listed there are the values of $v \sin i$ taken from the fourth edition of the *Bright Star Catalogue* (Hoffleit 1982).

Nissen (1981) has done a study of microturbulence in F and G stars and derives a relationship for microturbulent velocity based on T_e and $\log g$. For our sample of stars we find values of ξ between 1.5 and 2.1 km s^{-1} based on Nissen's work. Rather than calculate individual curves of growth for so many stars, we took the mean temperature (6460 K) and mean surface gravity (4.1) with Nissen's relationship for an average ξ of 1.8 km s^{-1} as the appropriate value for this sample of stars.

c) Abundances

A model atmosphere abundance analysis program was used to predict equivalent widths and line profiles for a given model atmosphere, microturbulent velocity, and array of abundances for specified lines or line blends. (This program is an outgrowth of one developed at Meudon primarily by Dr. M. Spite and Dr. F. Praderie and modified by Dr. W. D. Heacox at UH.) A grid of model atmospheres of Kurucz (1979) with solar metallicity were used. Abundances were calculated for Li I $\lambda 6707$, Ca I $\lambda 6717$, and Fe I $\lambda\lambda 6678, 6703, 6705, 6726$, and 6750 for the solar atmosphere ($T_e = 5770$ K) and for both $\log g = 4.5$ and 4.0 at values of $T_e = 6000, 6500, 7000$, and 7500 K. With the appropriate input parameters the influence of thermal and microturbulent broadening, radiation damping, van der Waals broadening, etc. are included in the calculations.

The gf -values for the Li I blend was taken from Gaupp, Kuske, and Andra (1982), for the Ca I line from Wiese, Smith and Miles (1969), for the Fe I lines from Blackwell *et al.* (1982), Gurtovenko and Kostik (1981), or Rutten and vander Zalm (1984). The Li I line is blended with a weak (5 mÅ in the Sun) Fe I line at 6707.441 Å; for this line we have used the astrophysical gf -value of Andersen, Gustafsson, and Lambert (1984). Even though the Fe I line is weak and has a vanishingly small effect on the Li abundance in the majority of stars, it is important to take it into account where the Li line is weak or absent. Therefore we calculated Li abundances at all temperatures and gravities for a Li-only feature and for Li-Fe blend with a range of Fe abundances: $[\text{Fe}/\text{H}] = -0.6, -0.3, 0.0$, and 0.3. For each of the Ca I and Fe I lines for each of the atmospheres, equivalent widths were calculated for seven abundances in steps of factors of 2 centered on the solar abundance. For all the Li calculations there were 10 input abundances starting at $\log \text{Li}/\text{H} = 10^{-13}$ and increasing by factors of 3 up to

TABLE 3
PHOTOMETRY AND STELLAR PARAMETERS

HR	m_1	c_1	$b-y$	β	$v \sin i$	T_e	$\log g$	M_v	$\log \text{age}$	HR	m_1	c_1	$b-y$	β	$v \sin i$	T_e	$\log g$	M_v	$\log \text{age}$
3579...	0.173	0.499	0.286	2.670	...	6580/5520	(4.1)	6467...	0.118	0.469	0.294	2.656	≤ 15	6340	4.0	3.14	9.4
3857...	0.162	0.594	0.244	2.696	12	6760	4.0	2.60	9.15	6489...	0.154	0.498	0.294	2.644	8	6225	3.8	2.71	9.6
3954...	0.169	0.478	0.318	2.651	10	6290	3.9	2.98	9.5	6541...	0.148	0.471	0.328	2.631	≤ 10	6105	3.8	3.90	9.6
3979...	0.165	0.490	0.286	2.676	8	6545	4.2	3.18	9.15	6569...	0.146	0.485	0.268	2.666	0	6440	4.1	3.10	9.3
4090...	0.195	0.956	0.151	2.774	31	7260 ^a	6594...	0.155	0.541	0.258	2.680	30	6585	4.0	2.74	9.3
4150...	0.136	0.476	0.289	2.639	8	6180	3.8	2.91	9.6	6595...	0.150	0.413	0.301	2.648	0	6265	4.2	3.63	ZAMS
4230...	0.132	0.580	0.264	2.670	...	6840/6750	(3.7)	6596...	6725/6755
4408...	0.155	0.594	0.251	2.679	30	6575	3.8	2.19	9.3	6600...	0.152	0.501	0.252	2.690	≤ 15	6695	4.3	3.32	ZAMS
4421...	0.124	0.494	0.268	2.655	...	6330	3.9	2.86	9.5	6670...	0.172	0.458	0.278	2.662	30	6400	4.1	3.32	9.3
4431...	0.148	0.429	0.340	2.628	≤ 6	6075	3.9	3.33	9.75	6734...	0.170	0.587	0.252	2.694	25	6585	4.0	2.61	9.15
4455...	0.169	0.419	0.302	2.661	14	6390	4.3	3.70	ZAMS	6797...	0.164	0.452	0.305	2.638	≤ 10	6170	3.9	3.15	9.6
4501...	0.125	0.400	0.310	2.632	≤ 10	6035	4.0	3.60	9.75	6844...	0.160	0.692	0.200	2.740	≤ 15	6977 ^c
4600...	0.143	0.497	0.276	2.661	0	6390	4.0	2.91	9.35	6850...	0.143	0.472	0.281	2.653	8	6310	4.0	3.06	9.45
4657...	0.115	0.328	0.320	2.612	8	5935	4.2	4.32	ZAMS	6985...	0.150	0.524	0.262	2.687	...	6775/6425	(4.2)
4803...	0.166	0.646	0.221	2.703	0	6790 ^a	3.9	2.26	UMa	7000...	0.140	0.569	0.299	2.664	...	7265/7595	(3.7)
4825...	0.168	0.714	0.195	2.809	28	6795 ^a	7163...	0.166	0.479	0.307	2.628	≤ 10	6075	3.7	2.84	9.65
4826...	0.166	0.525	0.235	2.690	30	6694	4.2	3.09	ZAMS	7247...	0.154	0.497	0.263	...	15	6595 ^b	4.2	3.28	ZAMS:
4914...	0.154	0.574	0.228	2.719	...	6455 ^a	4.3	3.20	ZAMS	7322...	0.147	0.435	0.320	2.640	≤ 6	6190	4.0	3.35	9.6
4926...	0.178	0.446	0.288	2.659	20	6370	4.2	3.40	9.35	7354...	0.125	0.425	0.320	2.646	12	6245	4.1	3.49	9.4
4934...	0.167	0.479	0.275	2.676	≤ 6	6545	4.2	3.29	ZAMS	7496...	0.161	0.507	0.295	2.661	21	6390	3.9	2.81	9.3
4946...	0.153	0.514	0.269	2.678	30	6565	4.1	2.97	9.2	7697...	0.156	0.507	0.280	2.679	≤ 10	6575	4.1	3.05	9.2
5074...	0.166	0.559	0.248	2.688	21	6670	4.0	2.73	9.2	7727...	0.186	0.464	0.334	2.633	≤ 10	6125	3.8	2.99	9.6
5075...	0.165	0.517	0.257	2.672	≤ 30	6500	4.0	2.85	9.3	7756...	0.164	0.481	0.281	2.671	≤ 10	6490	4.1	3.20	9.3
5110...	0.160	0.674	0.264	4345/6440	7925...	0.140	0.459	0.302	2.667	30	6450	4.2	3.38	ZAMS
5156...	0.146	0.464	0.278	2.663	12	6410	4.1	3.28	9.3	7936...	0.157	0.481	0.271	2.670	37	6480	4.1	3.19	9.3
5347...	0.144	0.522	0.255	2.679	≤ 6	6575	4.1	2.90	9.2	7973...	0.136	0.419	0.302	2.652	≤ 10	6300	4.2	3.60	ZAMS
5387...	0.161	0.488	0.261	2.685	8	6640	4.3	3.35	ZAMS	8205...	0.165	0.471	0.300	2.676	12	6545	4.2	3.37	ZAMS
5445...	0.131	0.476	0.300	2.657	12	6350	4.0	3.07	9.4	8222...	0.162	0.650	0.275	2.678	≤ 15	6565	3.6	1.63	9.15
5455...	0.136	0.457	0.316	2.638	15	6170	3.9	3.10	9.6	8354...	0.108	0.439	0.309	2.640	≤ 6	6190	4.0	3.31	9.6
5529...	0.139	0.518	0.258	2.678	12	6380	4.1	2.93	9.2	8400...	0.141	0.478	0.311	2.636	26	6150	3.8	2.86	9.6
5533...	0.169	0.491	0.313	2.660	20	6380	4.0	2.96	9.45	8507...	0.172	0.462	0.278	2.653	12	6310	4.0	3.17	9.4
5758...	0.164	0.514	0.236	2.694	23	6740	4.3	3.29	ZAMS	8514...	0.148	0.409	0.302	2.620	7	6005	4.0	3.49	9.75
6052...	0.152	0.576	0.247	...	30	6715 ^b	4.1	2.84	9.15	8805...	0.152	0.495	0.286	2.672	9	6500	4.1	3.07	9.3
6181...	0.173	0.540	0.276	2.664	30	6420	3.8	2.52	9.4	8825...	0.145	0.442	0.302	2.640	18	6190	4.0	3.28	9.65
6189...	0.133	0.393	0.320	2.613	≤ 15	5945	4.0	3.61	9.85	8885...	0.170	0.489	0.296	2.663	12	6410	4.0	3.02	9.3
6193...	0.205	0.893	0.110	2.822	34	7685 ^a	8907...	0.163	0.543	0.281	2.687	0	6660	4.1	2.86	9.4
6290...	0.190	0.723	0.208	2.709	23	6797 ^c	3.7	1.69	9.15	8977...	0.154	0.514	0.272	2.683	30	6620	4.1	3.06	9.2
6445...	0.149	0.501	0.253	2.681	0	6595	4.2	3.15	9.15										

^a T_e from (R-I) Hearnshaw 1974 calibration.

^b β calculated from $b-y$.

^c β to (R-I) from Crawford 1978.

TABLE 4
DATA FOR SPECTROSCOPIC BINARIES

HR	$W(6703)$	T_e (K)	$B_r(b)$	mf
	$W(6705)$		$B_r(r)$	
3579 ^a b.....	...	6580	1.905	{1.24 5.11}
r.....	...	5520		
4230 b.....	0.366	6840	1.045	{1.93 2.07}
r.....	0.397	6750		
5110 ^b b.....	1.225	4345	0.195	{15.3 1.07}
r.....	0.503	6440		
6596 ^c b.....	0.406	6725	0.985	{2.02 1.98}
r.....	0.395	6755		
6985 b.....	0.388	6755	1.185	{1.70 2.43}
r.....	0.509	6425		
7000 b.....	0.219	7265	0.873	{2.25 1.80}
r.....	0.105	7595		

^a HR 3579—Temperatures from spectral types F5 V and G5 V and masses, 1.13 and 0.84 M_\odot .

^b HE 5110—No abundances done for the cool component. The line in that component at 6707 is all Fe I, not Li I.

^c HR 6596—Since 6703r and 6705b are blended, we took 6727b = 6705b which is empirically true in general since the two lines are from the same multiplet and have the same excitation potential.

2×10^{-9} . From these calculations curves of growth could be constructed and abundances could be interpolated at the appropriate temperature and gravity at the measured equivalent width for each star. An example of one set of these curves is shown in Figure 4 for the Li-only feature and in Figure 5 for the Li-Fe blend for $[\text{Fe}/\text{H}] = 0.0$. The Li line strength is not sensitive to either $\log g$ or ξ , nor are any of the other lines except Fe I $\lambda 6678$ very sensitive to $\log g$ or ξ . In those cases where the abundance found from Fe I $\lambda 6678$ was very different (≥ 0.2 – 0.3 dex) from that found from the other lines, it was not included in the average Fe/H abundance; that line is almost always on the flat portion of the curve of growth and thus the abundance is very sensitive to the measured equivalent width also.

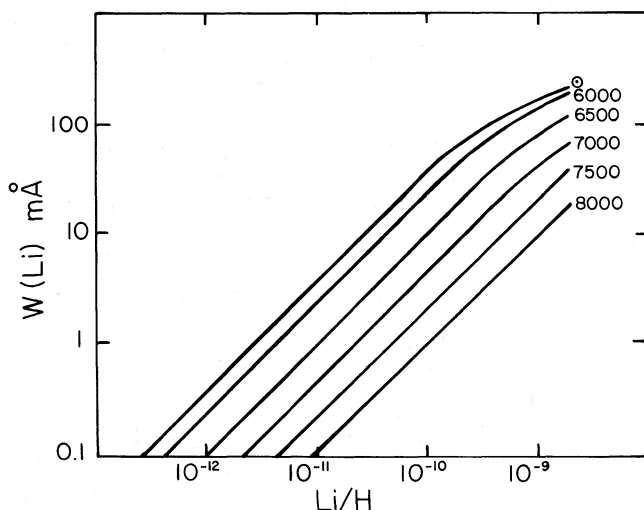


FIG. 4.—Sample curves of growth for the Li I $\lambda 6707$ feature for several different temperatures from Kurucz model atmospheres. The $\log g$ value is 4.5 for this set of curves and the microturbulence is 1.8 km s^{-1} but 1.2 km s^{-1} for the Sun.

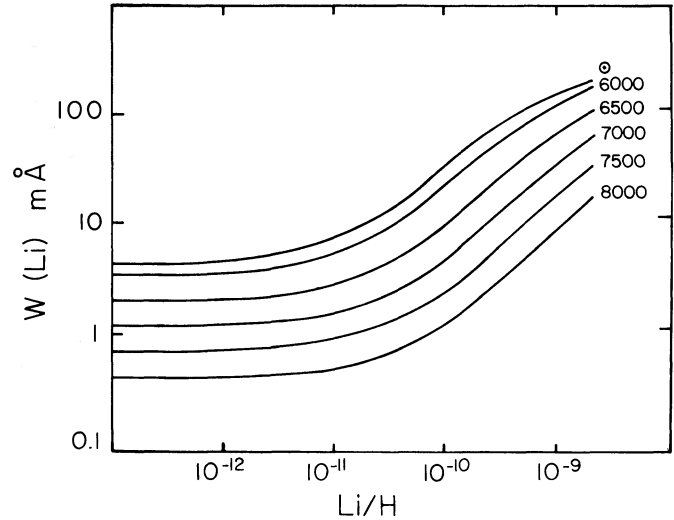


FIG. 5.—Sample curves of growth for the Li I-Fe I blend, analogous to Fig. 4. Here $[\text{Fe}/\text{H}]$ is 0.0, but additional curves were calculated for -0.6 , -0.3 , and $+0.3$.

Solar abundances were determined through use of Kurucz's (1979) solar atmosphere and the equivalent widths in the Utrecht solar atlas (Moore, Minnaert, and Houtgast 1966). The value used for the solar microturbulence was that of Blackwell *et al.* (1976) for the integrated solar disk: 1.2 km s^{-1} . The resultant $(\text{Fe}/\text{H})_\odot = 2.70 \times 10^{-5}$, in good agreement with the value of 2.63×10^{-5} found by Blackwell *et al.* with the Kurucz atmosphere, $\xi = 1.2 \text{ km s}^{-1}$, and a different set of Fe I lines. The solar Ca/H abundance found from the one strong Ca I line with a poorly known gf -value is 3.9×10^{-6} , in less good agreement with the Lambert and Luck (1978) solar Ca/H of 2.19×10^{-6} . In order to minimize the effect of the gf -values on the stellar abundances, a stellar-to-solar ratio was found for each line, thence $[\text{Fe}/\text{H}]$ and $[\text{Ca}/\text{H}]$. No solar Li/H was determined so stellar Li abundances are given as $\log N(\text{Li})$ where $\log N(\text{H}) = 12.00$.

The final abundances from the equivalent widths in Table 2, the atmospheric parameters in Table 3, and the calculated curves of growth are presented in Table 5.

IV. RESULTS AND DISCUSSION

a) Population I "Initial" Lithium

Although there is no theoretical expectation for any Li depletion in early F stars, even a cursory look at Table 5 reveals a range of Li abundances of over two orders of magnitude. About one-third of the stars have the anticipated initial abundance of $\text{Li}/\text{H} = 10^{-9}$, and these are preferentially the hotter ones in the sample. The position of the stars in the H-R diagram (from the Strömgren photometry which yielded the parameters M_v and T_e given in Table 3) is shown in Figure 6 where the three different symbols correspond to three different Li abundance ranges. The filled circles representing stars with $\log N(\text{Li}) \geq 2.5$ appear predominantly in the hotter part of the diagram. These higher Li abundances account for 82% of the stars hotter than 6650 K, for 41% in the temperature range 6450–6650 K, but only 12% and 13%, respectively, in the ranges 6250–6450 K and less than 6250 K. (Throughout this temperature range Li is highly ionized, but the degree of ionization does not change much from 6000 to 7000 K; the values

TABLE 5
ABUNDANCE RESULTS

HR	log N(Li)	[Fe/H]	[Ca/H]	HR	log N(Li)	[Fe/H]	[Ca/H]
3579.....	≤ 1.5/2.2:	-0.3/...	-1.1/...	6467.....	≤ 1.20	-0.41	-0.46
3857.....	1.86	+0.14	+0.19	6489.....	2.93	-0.17	-0.14
3954.....	2.00	+0.07	+0.19	6541.....	≤ 1.36	-0.22	-0.11
3979.....	2.73	+0.19	+0.34	6569.....	≤ 1.10	-0.25	-0.19
4090.....	...	+0.16 ^a	+0.31	6594.....	2.40	-0.13	+0.11
4150.....	...	-0.33	-0.25	6595.....	2.26	-0.17 ^a	-0.16
4230.....	2.2/1.5	-0.1/-0.2	-0.1/+0.2	6596.....	3.5/3.1	+0.4 ^a /0.0	.../-0.1
4408.....	2.95	-0.20	-0.29	6600.....	≤ 1.13	-0.17	-0.14
4421.....	≤ 1.26	-0.61	-0.57	6670.....	≤ 1.08	+0.10	+0.09
4431.....	2.49	-0.32	-0.29	6734.....	3.15	0.07	0.02
4455.....	2.66	+0.12	+0.23	6797.....	≤ 1.32	-0.22	-0.11
4501.....	≤ 0.90	-0.82 ^a	-0.71	6844.....	3.11	+0.17	+0.15
4600.....	≤ 1.28	-0.21	-0.13	6850.....	≤ 1.28	-0.17	-0.15
4657.....	≤ 1.34	-0.77	-0.66	6985.....	3.1/≤ 1.7	+0.1/0.0	+0.1/+0.1
4803.....	3.04	-0.17 ^a	+0.15	7000.....	~ 3.3/~ 3.3:	+0.1 ^a /+0.3 ^a	+0.3/...
4825.....	3.00	-0.07 ^a	-0.21	7163.....	2.64	-0.19	+0.01
4826.....	3.00	-0.07	-0.18	7247.....	3.15	0.00	+0.08
4914.....	2.63	-0.30	-0.21	7322.....	≤ 1.02	-0.28	-0.21
4926.....	≤ 1.57	+0.10	+0.28	7354.....	1.32	-0.19	-0.10
4934.....	≤ 1.52	+0.07	+0.21	7496.....	≤ 1.30	+0.09	-0.28
4946.....	3.00	-0.19	-0.16	7697.....	...	+0.11	+0.24
5074.....	3.15	+0.06	+0.14	7727.....	≤ 1.34	0.00	+0.19
5075.....	≤ 0.48	-0.04	+0.12	7756.....	≤ 1.32	+0.03	+0.07
5110.....	.../...	.../-0.3	.../-0.3	7925.....	≤ 1.36	+0.03	+0.16
5156.....	≤ 1.00	-0.20	-0.19	7936.....	≤ 1.18	+0.04	+0.01
5347.....	2.87	-0.17	-0.23	7973.....	2.11	-0.22	-0.14
5387.....	≤ 1.61	0.00	+0.04	8205.....	2.38	+0.17	+0.45
5445.....	≤ 1.15	-0.11	-0.07	8222.....	2.87	+0.05	+0.16
5455.....	≤ 1.38	-0.22	-0.06	8354.....	1.65	-0.59	-0.36
5529.....	≤ 1.06	-0.39	-0.25	8400.....	1.98	-0.24	-0.18
5533.....	1.78	+0.08	+0.12	8507.....	≤ 1.34	+0.02	+0.01
5758.....	2.92	+0.01	-0.06	8514.....	2.00	-0.39	-0.16
6052.....	2.73	+0.01	+0.07	8805.....	≤ 0.90	-0.07	+0.03
6181.....	2.52	+0.05 ^a	+0.31	8825.....	≤ 1.15	-0.27	-0.16
6189.....	2.20	-0.63 ^a	-0.61	8885.....	1.72	+0.05	+0.02
6193.....	3.25	-0.08	+0.19	8907.....	3.04	-0.15	-0.07
6290.....	2.83	-0.13 ^a	+0.28	8977.....	≤ 1.41	+0.17	+0.31
6445.....	≤ 1.68	-0.19	-0.25				

^a Fe I line $\lambda 6678$ omitted from mean [Fe/H].

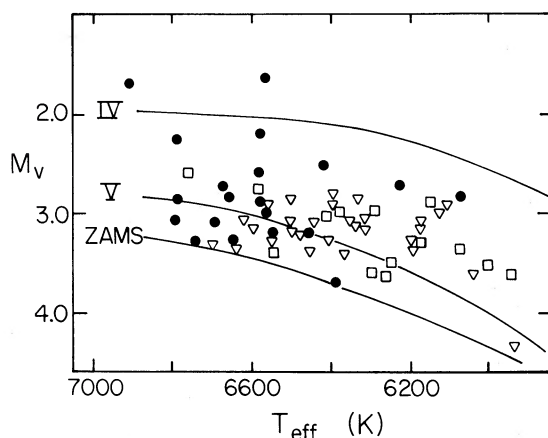


FIG. 6.—The distribution of single F stars observed for Li for which Ström-gren photometry was available to convert to the H-R diagram parameters, M_V and T_{eff} . The filled circles have $\log N(\text{Li}) \geq 2.5$; the open squares correspond to points with $\log N(\text{Li}) < 2.5$ and generally > 1.7 while the downward-pointed triangles indicate upper limit values for $\log N(\text{Li})$, which are typically ≤ 1.7 to ≤ 0.9 . The solid lines show the location of the zero-age main sequence (ZAMS), the range to luminosity class V and class IV stars according to the calibration of Crawford (1975). Note the preponderance of high Li stars (the solid circles) in the hotter part of the diagram.

for $\text{Li I}/\text{Li}$ at $\tau = 1$ are 1.0×10^{-3} for 6000 K, 9.6×10^{-4} for 6500 K, and 8.8×10^{-4} at 7000 K for models with $\log g = 4.5$.)

Figure 7 details the Li abundance relationship with stellar surface temperature ($T_e \equiv T_{\text{eff}}$). Although about one-third of the stars show the “cosmic” Li abundance, 15% are depleted by factors of 3–10 and 52% by 10 to up to at least a factor of 150! There are 18 stars hotter than $T_e = 6500$ K which appear to contain their original Li content. For these

$$\langle \text{Li}/\text{H} \rangle = 1.02(\pm 0.34) \times 10^{-9}, \quad \text{or} \quad \langle \log N(\text{Li}) \rangle = 3.01.$$

For these higher temperature stars there appears to be a dichotomy in the Li content: most have cosmic Li, but a few have only upper limits with abundances down from $\text{Li}/\text{H} = 10^{-9}$ by factors of 20–120. These Li-depleted stars are reminiscent of the large depletions we have found in a narrow temperature span in Hyades F dwarfs (Boesgaard and Tripicco 1986). Between $T_e = 6000$ –6500 K there are stars with values over the whole range of Li/H , but 78% have $\log N(\text{Li}) < 2.0$.

b) Lithium and Age in F Dwarfs

The connection of Li abundance and age in this sample of stars can be investigated in a variety of ways. Included in our

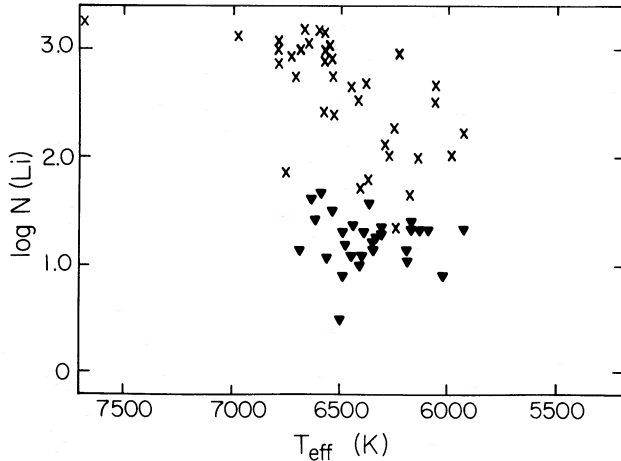


FIG. 7.—Lithium abundances on the scale where $\log N(\text{H}) = 12.0$ for all of the stars except the double-lined spectroscopic binaries as a function of effective temperature. The crosses are for measured abundances while the downward-pointed filled triangles are for upper limit values. The Sun would appear at (5770, 1.0). For stars cooler than about 6500 K there are points over the whole range of Li abundances, but for those hotter than 6500 K there appears to be a dichotomy in the values with most stars having $\log N(\text{Li})$ near 3.0.

sample is a star that we know to be young: HR 4803 in the UMa stream (Roman 1949; Eggen 1960) that is thought to have an age of 2.7×10^8 yr (Giannuzzi 1979). This star has $\log N(\text{Li}) = 3.04$ which lends strength to the generally observed inverse relation between Li abundance and age (e.g., Duncan 1981). Soderblom (1985) reports on two other UMa stream stars, HR 6748 and HR 6098, that fit this pattern with temperatures and $\log N(\text{Li})$ values of 5850 K, 2.81 and 6100 K, 3.05 respectively.

As a method of sorting out the oldest stars in our sample we calculated space velocities, U , V , and W , to find those which are “high-velocity” stars according to the criteria of Oort (1926): $|W + 10| \geq 30 \text{ km s}^{-1}$ and/or $(U^2 + V^2)^{1/2} \geq 65 \text{ km s}^{-1}$. We give here the specifics of this calculation since it is not readily accessible in the astronomical literature in a convenient form. The relevant equations and numerical coefficients are

$$U = -0.06715X - 0.87272Y - 0.48359Z,$$

$$V = 0.49274X - 0.45040Y + 0.74454Z,$$

and

$$W = -0.86760X - 0.18837Y + 0.46020Z,$$

where X , Y , and Z are given by the following expressions

$$X = -C\mu_\alpha \sin \alpha - C\mu_\delta \cos \alpha \sin \delta + V_r \cos \alpha \cos \delta + 0.2$$

$$Y = C\mu_\alpha \cos \alpha - C\mu_\delta \sin \alpha \sin \delta + V_r \sin \alpha \cos \delta - 17.2$$

$$Z = C\mu_\delta \cos \delta + V_r \sin \delta + 9.6.$$

In the last set of equations, $C = 4.738/p$, where p is the parallax in arc seconds, α and δ are the right ascension and declination for 1950.0, μ_α and μ_δ are the components of proper motion in arc seconds yr^{-1} in right ascension and declination respectively, V_r is the heliocentric radial velocity in km s^{-1} . The constants at the end of the expressions for X , Y , and Z take out the standard solar motion, 19.7 km s^{-1} toward $\alpha = 270.6$ and $\delta = 29.2$. The U , V , W velocities are in km s^{-1} and U is in the galactic plane and positive toward $l = 0$, $b = 0$, V is positive

toward $l = 90$, $b = 0$ (toward the direction of rotation) and W is positive toward the north galactic pole. All our input parameters were taken from the Fourth Edition of the Bright Star Catalog (Hoffliet 1982). We also observed a number of stars studied by Eggen (1972) who calculated space motions for metal-deficient F stars. (We note that his U velocities have the opposite sign from our convention.)

Table 6 lists the U , V , W velocities (an E indicates those taken from Eggen with the sign for the U velocity changed), the values of $(U^2 + V^2)^{1/2}$ and $|W + 10|$, and for the genuine high-velocity objects the values of $\log N(\text{Li})$ and $[\text{Fe}/\text{H}]$. None of the eight high-velocity stars (or the two on the borderline) showed a detectable Li I feature and the abundances are upper limits, typically two orders of magnitude lower than the “cosmic” value. With one or two exceptions they also are metal-deficient with $-0.8 \leq [\text{Fe}/\text{H}] \leq -0.2$. The dependence of Li on age appears to be upheld by this sample of old disk F dwarfs which are so deficient in Li, presumably because they have been slowly depleting their surface Li (for example by diffusion or convective overshoot) as they age.

In their study of Li in halo stars and old disk late F and G stars Spite and Spite (1982) propose that Li is gradually enriched over the lifetime of the galaxy with $\log N(\text{Li}) \approx 2.0$ in the very old halo stars, ≈ 2.5 in the old disk stars, and ≈ 3.0 in the present interstellar gas (see their Fig. 6). Our old disk F stars show no indication of such enrichment since our upper limits on $\log N(\text{Li})$ are typically $\lesssim 1.0$. For the F dwarfs the kinematic age indicator agrees with the Li age indicator and not with a picture of general galactic Li enrichment. However, these F stars ($M \approx 1.3\text{--}1.7 M_\odot$) do have shallower convection zones than the Spites’ G stars ($M \approx 0.8 M_\odot$) so should be even less susceptible to the standard convective depletion than similar metallicity G dwarfs.

As discussed in § IIIb, for the stars with published Strömgen photometric indices we could estimate the age unless $\delta c_1 \leq 0.03$. The individual ages are presented in Table 3.² In Figure 8 the Li abundances are shown as a function of these ages for stars with $-0.3 < [\text{Fe}/\text{H}] < +0.3$. (The true age from the isochrones will be influenced by the metallicity of the individual star and by limiting our sample to solar metallicity we can reduce this source of uncertainty.) The maximum $\log N(\text{Li})$ is about 3.0 for the youngest stars—those with $\log \text{age} \leq 9.3$ —and 79% of those stars have $\log N(\text{Li}) > 2.0$. Although there is a spread in Li abundance at all ages, there is an upper bound for stars older than 2×10^9 yr such that the maximum Li decreases with increasing age. Two-thirds of the F stars with the Sun’s age ($\log \text{age} = 9.65$) have depletions similar to that in the Sun so the Sun is *not* unique for its age.

The real message of Figure 8 can be seen by the histograms in Figure 9 which show a completely different distribution of Li abundance in stars younger than 2×10^9 and those with ages $\geq 2 \times 10^9$. (The Li abundances are more accurately determined than the ages so such a coarse division into two age groups is probably warranted.) In the “young” star group 62% have $\log N(\text{Li}) = 2.6\text{--}3.2$. In the “old” star group 77% have $\log N(\text{Li}) \leq 2.0$ and 64% have $\log N(\text{Li}) \leq 1.4$ or deficiencies of factors of 40 or more. [Recall that $\log N(\text{Li})$ of 2.0 is the Li content of the typical G dwarfs in the halo population where ages are more like $10\text{--}15 \times 10^9$ yr.] There are only two

² Representative main sequence lifetimes for F0 V ($1.7 M_\odot$) and F5 V ($1.3 M_\odot$) are 2.5×10^9 and 4.7×10^9 yrs respectively, or $\log \tau = 9.4$ and 9.7 .

TABLE 6
 SPACE VELOCITIES

HR	U	V	W	$(U^2 + V^2)^{1/2}$	$ W + 10 $	$\log N(\text{Li})$	[Fe/H]	Source ^a
3579.....	-30	-1	1	30	11	
4150.....	21	-6	-16	22	6	E
4408.....	33	-21	4	39	14	E
4421.....	-24	28	-38	37	28	E
4431.....	-2	8	-34	8	24	E
4455.....	-1	-3	0	3	10	
4501.....	-55	-9	21	56	31	≤ 0.90	-0.82	
4600.....	63	-1	13	63	23	≤ 1.28	-0.21	
4657.....	81	-81	-72	115	62	≤ 1.34	-0.77	
4803.....	22	15	-3	27	7	
4825.....	-17	9	-11	19	1	
4826.....	-17	9	-11	19	1	
4914.....	-30	0	+3	30	13	
4926.....	-41	-4	12	41	22	
4934.....	-10	-3	-2	10	8	
4946.....	5	2	8	5	18	
5110.....	26	25	12	36	22	
5156.....	-26	-25	3	36	13	
5347.....	-30	-31	-11	43	1	E
5445.....	14	15	-18	20	8	E
5455.....	-121	-7	32	121	42	≤ 1.38	-0.22	
5529.....	-51	-22	-1	56	9	≤ 1.06	-0.39	
6052.....	21	17	-13	27	3	
6445.....	5	11	-18	12	8	
6467.....	43	106	-78	114	68	≤ 1.20	-0.41	E
6541.....	-19	-31	-19	36	9	
6569.....	8	4	-10	9	0	
6594.....	-30	-3	-5	30	5	
6595.....	22	9	13	24	23	
6596.....	-21	0	-3	21	7	
6670.....	-21	-3	16	21	26	
6734.....	-26	0	-1	26	9	
6797.....	10	-7	-7	12	3	
6850.....	6	-1	-37	6	27	
6985.....	5	-11	-2	12	8	
7322.....	-68	-22	29	72	39	≤ 1.02	-0.28	
7496.....	20	7	-18	21	8	
7697.....	-50	-21	-9	54	1	
7727.....	-9	1	-5	9	5	
7925.....	-22	-6	+28	23	38	≤ 1.36	+0.03	
7936.....	33	15	-8	36	2	
7973.....	-4	27	9	27	19	
8205.....	16	3	-22	16	12	
8354.....	23	31	0	39	10	
8400.....	37	6	-8	38	2	
8514.....	-6	8	-8	9	2	E
8805.....	-32	4	23	33	33	≤ 0.90	-0.07	
8825.....	72	-17	1	74	11	≤ 1.15	-0.27	

^a E = Eggen 1972.

F0–F5 dwarfs older than 3×10^9 yr with $\log N(\text{Li}) > 2.0$. (These two stars, HR 6489 and HR 7163—the spectrum of the latter is shown in Fig. 1—are mildly metal-deficient, slow rotators with Ca II activity index, $\log R'_{\text{HK}}$, more appropriate for the low Li group in Fig. 12, § IVd below.) In a complementary study (Boesgaard and Tripicco 1985), we have determined Li abundances in 25 F0–G0 dwarfs in visual binaries for which Duncan (1984) has found ages by use of Strömgren photometry and isochrones. Most of those stars have ages between log age = 8.9 and 9.3 and values of $\log N(\text{Li})$ between 2.0 and 3.0. The addition of those stars to this sample reinforces the general trend of a Li decline with age for F stars, but with a typical spread of an order of magnitude in Li. When Li abundances are compared to ages found by isochrones, we see only a statistical connection and it appears that other stellar or galactic characteristics influence the Li content.

A dependency of depletion upon age is further bolstered by the fact that in the Hyades and Pleiades in the T_e range 6000–6400 K, these young stars have $\log N(\text{Li})$ values near the 3.0 maximum (Duncan and Jones 1983). In contrast the early F stars in the field are generally older than the Hyades but in this temperature range they show moderate to substantial depletions of Li.

c) Lithium and Metallicity

It has been suggested by Spite and Spite (1982) that the halo stars contain the Li abundance inherited from Big Bang nucleosynthesis and that the galactic disk has been gradually enriched in Li over time so that the present disk content of Li is an order of magnitude greater than what it was at the time of the formation of the halo stars. If this is the case, an old, i.e., metal-deficient, F star in the disk should have inherited a lower

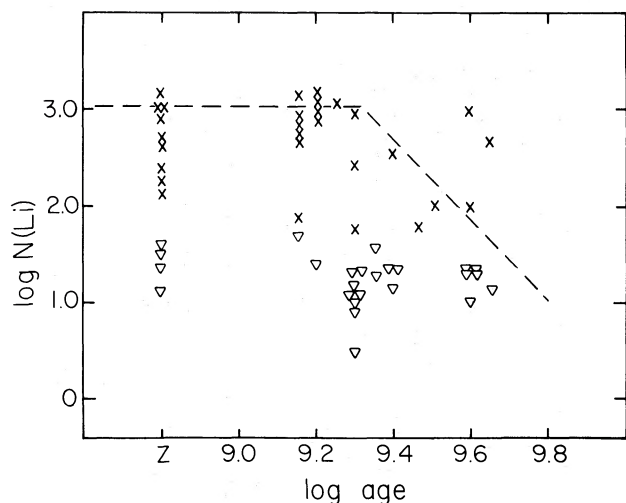


FIG. 8.—Lithium abundances vs. age in those stars for which age estimates can be made from Strömgren photometry and isochrones. The points plotted at Z are those too near to the zero-age main sequence to be dated reliably. The stars in this plot are in the metallicity range $-0.3 < [\text{Fe}/\text{H}] < +0.3$ in order to reduce the uncertainty in age due to metallicity differences. Again the crosses are measured Li abundances, while the triangles are upper limit values. The dashed line corresponds to a maximum to which most of the stars conform. If this figure is divided at $\log \text{age} = 9.3$ (2 billion years), it can be seen that the younger stars are mostly Li-rich while most of the older stars are Li-poor with only upper limit values. The Sun at (9.65, 1.0) is not unique for its age since two-thirds of the F stars show similar Li deficiencies to the solar one.

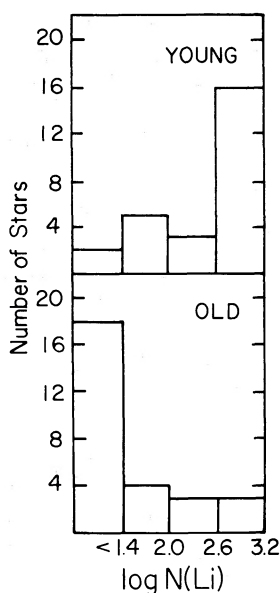


FIG. 9

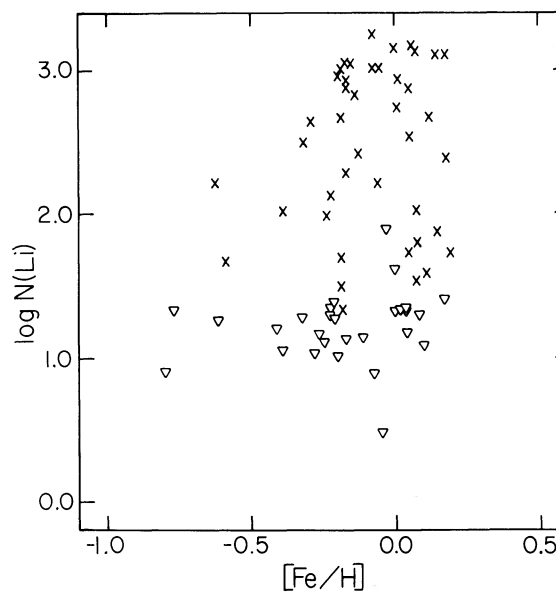


FIG. 10

FIG. 9.—The distribution of Li abundances in the stars in Fig. 8 for the two age groups where “young” means $< 2 \times 10^9$ yr and “old” means $\geq 2 \times 10^9$ yr. The distributions are opposite to each other with the young stars being predominantly Li-rich and the old stars, Li-poor. A range in Li abundance is seen in both age groups.

FIG. 10.—A comparison of the Li abundances with the logarithmic ratio of Fe/H relative to the solar Fe/H (i.e., $[\text{Fe}/\text{H}]$) determined from the same spectroscopic data and model atmospheres as the Li results. The triangles represent upper limits on the Li abundances. There is an absence of points in the upper left, or an absence of stars that are Li-rich and metal-poor. All of the stars with $\log N(\text{Li})$ near 3.0 have solar metallicity. But at solar metallicity ($-0.2 < [\text{Fe}/\text{H}] < +0.2$) there is a rather uniform distribution of all Li abundance values. There is a greater spread in metallicity at low (~ 1.0) Li abundance. Although they represent a different group of stars, it could be noted that the low-mass Population II G stars discussed by Spite *et al.* (1984) would be clustered near $\log N(\text{Li}) = 2.0$ but off to the left of this figure from $[\text{Fe}/\text{H}] = -1.0$ to -2.2 .

content of Li at the time of formation than a disk star with solar metallicity. (See Twarog 1980 for the evidence of the relation of metallicity with age in the galactic disk.) On the other hand, individual late F and G stars slowly destroy their Li during main-sequence evolution according to Duncan (1981) and others. This implies that the old disk stars, old as evidenced by their low metallicity, would contain a reduced Li abundance because they inherited less and they have had more time to destroy it. Whether one or both of these effects operates in the early F stars or which might dominate is not clear, but see the discussion in § IVb, above, which describes the severe lack of Li in the old disk F stars. On the other hand, there are indications from both theory (D’Antona and Mazzitelli 1984) and observation (Spite and Spite 1982) that stars with lower metallicity have shallower convection zones for a given T_e and thus destroy Li less readily than solar metallicity stars. Thus, the competition between (1) the greater age which leads to greater depletion because of the longer time scale and (2) the lower metallicity which means less depletion because of the slower losses via convective mixing may contribute a spread in the Li versus Fe diagram.

With our sample of F stars we can look at the empirical relation between Li and metallicity. We determined $[\text{Fe}/\text{H}]$ abundances which are listed in Table 5. These results are shown in Figure 10. No compelling pattern emerges from this figure, but there is an absence of stars with high Li [$\log N(\text{Li}) > 2.5$] and metallicity less than 2 times below solar ($[\text{Fe}/\text{H}] < -0.3$). In fact the whole upper left triangle from $(-1.0, 1.0)$ to $(-0.2, 3.0)$ is virtually devoid of points. [But note that the halo stars of Spite, Maillard, and Spite 1984 would lie

at $\log N(\text{Li}) = 2.0$ at metallicities off the left of this plot with $[\text{Fe}/\text{H}]$ from -1.0 to -2.2 .] At high $\log N(\text{Li})$ values (~ 3.0), all the stars have solar metallicity, while for stars with low $\log N(\text{Li})$ upper limits (~ 1.0), there is a greater range in metallicity. At values of $[\text{Fe}/\text{H}]$ between -0.2 and $+0.2$ there is an even distribution of the full range of values for $\log N(\text{Li})$. We can find stars with solar metallicity with values of the Li abundance which range over more than two orders of magnitude. Whether this range in Li results from different initial Li contents or slow depletion of Li with age, or both, cannot be discerned from these data. The absence of high-Li, low-metallicity objects can be accounted for by either idea.

Abundances were also determined for Ca. These are based on only one line and at high Ca/H abundances, that line is often on the flat portion of the curve of growth, so those abundances are less accurate than the ones for Fe or Li. The plot of $\log N(\text{Li})$ versus $[\text{Ca}/\text{H}]$ is very similar to that of $\log N(\text{Li})$ versus $[\text{Fe}/\text{H}]$ which is shown in Figure 10; there is the same absence of points in the upper left (at low Ca, but high Li) and the same spread of more than two orders of magnitude in Li values at Ca/H values within a factor of 2 of the solar value. In fact, the Ca and Fe abundances are well correlated which can be seen in Figure 11. A 45° slope can represent the data well if there is a shift of $\Delta[\text{Fe}/\text{H}]$ of about -0.1 dex, i.e., $[\text{Ca}/\text{Fe}] = +0.1$. Within the accuracy of the determinations, this is not particularly different from the recent results of Tomkin, Lambert, and Balachandran (1985) who suggest that $[\text{Ca}/\text{Fe}]$ is ~ 0.0 for $[\text{Fe}/\text{H}] \gtrsim -0.3$ and increases to $\sim +0.5$ for halo metallicities ($[\text{Fe}/\text{H}] \lesssim -1.0$), due to the greater synthesis of even- Z elements (Mg, Si, Ca) in the halo relative to Fe synthesis.

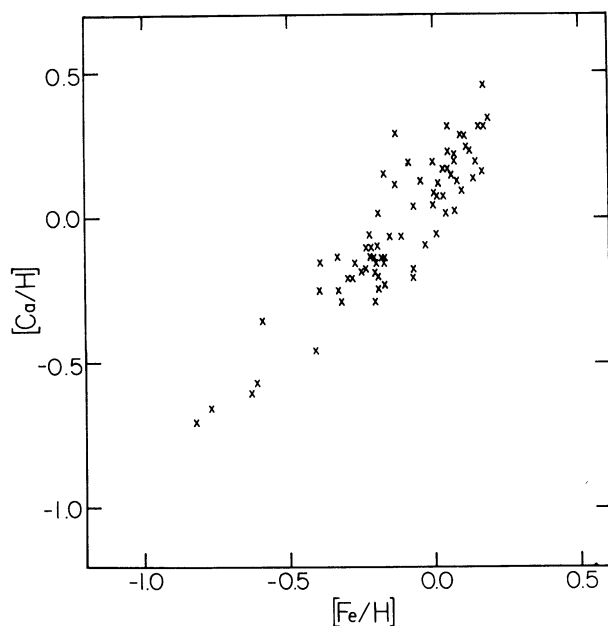


FIG. 11.—Logarithmic abundances relative to the Sun of Ca and Fe determined from the same data set and analysis. The two elemental abundances seem well correlated, but there may be a slight systematic shift of about -0.1 in $\Delta[\text{Fe}/\text{H}]$. At solar and higher metallicity the Ca abundances are somewhat suspect since they are based on one line which is near the flat portion of the curve of growth in strong-lined stars; this probably accounts for the upward drift of points from a 45° slope in the upper right.

TABLE 7
ACTIVITY AND ROTATION PERIODS

HR	S	$B-V$	$\log R'_{\text{HK}}$	$P_{\text{rot}}(\text{days})$
4455.....	0.20	0.46	-4.69	3.72
4657.....	0.21	0.46	-4.65	3.40
4825.....	0.23	0.36	-4.50	0.57
4826.....	0.29	0.36	-4.35	0.29
5445.....	0.21	0.40	-4.60	1.43
5533.....	0.17	0.48	-4.83	5.98
6181.....	0.23	(0.43) ^a	(-4.56) ^a	(1.84) ^a
6489.....	0.19	0.46	-4.73	4.06
6541.....	0.14	0.48	-5.04	7.48
6594.....	0.24	(0.38) ^a	(-4.48) ^a	(0.72) ^a
6596.....	0.21	0.43	-4.62	2.23:
6670.....	0.20	0.42	-4.65	2.13
6850.....	0.21	0.38	-4.57	1.00
6985.....	0.24	0.37	-4.48	0.61
7163.....	0.20	0.46	-4.69	3.72
7354.....	0.21	0.44	-4.63	2.59
7925.....	0.21	0.46	-4.65	3.40
8205.....	0.20	0.44	-4.67	2.84
8354.....	0.15	0.42	-4.90	3.28
8507.....	0.19	0.44	-4.71	3.12
8805.....	0.17	0.44	-4.80	3.69
8825.....	0.22	0.44	-4.90	4.19
8885.....	0.17	0.46	-4.82	4.78
8977.....	0.20	0.39	-4.62	1.32

^a Uncertain since the $B-V$ numbers were deduced from τ_c rather than measured.

d) Lithium and Activity

Twenty-four of our field F stars have been observed by the Mount Wilson HK project which measures the flux in a 1 \AA bandpass in the core of the Ca II H and K lines. A compilation of all the measurements and of the average S value was kindly provided to us by Ms. Laura Woodard. We have converted these measured S values to the proportion of the stellar chromospheric flux that appears in the Ca II H and K cores, R'_{HK} according to the prescriptions given by Noyes *et al.* (1984).

Table 7 gives the S values, $B-V$, and $\log R'_{\text{HK}}$ so determined for the stars in our sample which had been observed at Mount Wilson. The Li abundances are plotted against this activity index in Figure 12 for the 24 stars. It so happens that in the subsample where the Ca II HK index was measured, there appear to be two groups: the Li-rich and Li-poor stars. In Figure 12 the mean HK activity level for each group is indicated by a large circle. Although the error bars (1σ) of this mean overlap and activity, as measured by HK, is weak in F stars, there does appear to be a general trend with the Li-rich sample being the more active. In stars where *both* Li is high and activity is enhanced, this could be another reflection of stellar age. At an intermediate activity index of $\log R'_{\text{HK}} = -4.6$ one can see the full range of about two orders of magnitude in Li abundance.

Again by following the precepts of Noyes *et al.* (1984), we can calculate $\log(P_{\text{rot}}/\tau_c)$, where P_{rot}/τ_c is the Rossby number, i.e., the ratio of the rotation period to the convective turnover time. Noyes *et al.* (1984) use Gilman's (1980) calculations for τ_c and form an expression which is a function of $B-V$. Thus τ_c values can be calculated and P_{rot} values extracted from the measured R'_{HK} ; these values are also given in Table 7. For the Li-rich stars [$\log N(\text{Li}) > 2.4$] the mean $\langle P_{\text{rot}} \rangle = 2.1 \pm 1.6$ days. The stars in the Li-depleted group which have $\log N(\text{Li}) < 1.8$ have slightly slower rotation with $\langle P_{\text{rot}} \rangle = 3.3 \pm 1.7$, but again the error bars overlap.

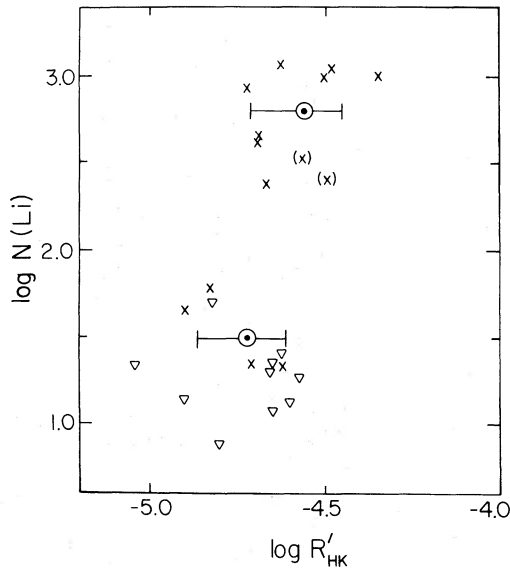


FIG. 12.—Li abundances in the subsample of stars for which Mount Wilson measures of the Ca II HK index were available as a function of the proportion of the stellar flux emitted in the cores of the Ca II resonance lines. The stars happen to fall into two groups: Li-rich and Li-poor. The mean of the numerical value of R'_{HK} for each group is plotted as the circled dot, and the 1σ error bars of the numerical mean are shown at the corresponding logarithmic values. The activity level in F stars as measured by Ca II HK is low so only a weak tendency toward the Li-activity connection is seen.

e) Lithium and Rotation

For solar-type stars, van den Heuvel and Conti (1971) found an exponential decay of Li with age and an exponential decline of rotation with age due to magnetic braking. Skumanich (1972) showed declines in Li abundance, chromospheric activity and rotation with age. For the early F stars there appears to be a Li-age connection but only a weak Li-activity connection at best. Here we examine the Li-rotation relationship.

Pseudo-rotation periods calculated from the Ca II HK flux and $B-V$ values (see Table 7) give the hint that the stars which have slowed down (presumably by magnetic braking) have depleted their Li, while the more rapidly rotating stars are Li-rich and probably young. Another means of looking at rotation is through the $v \sin i$ values that have been measured. These values were listed in Table 3. (The stars selected have

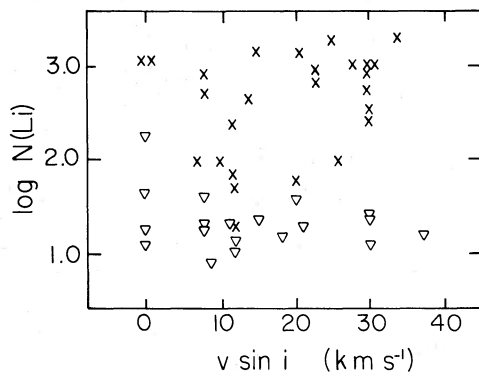


FIG. 13.—Li abundances against $v \sin i$ for those stars that have measured, as opposed to upper limit, values of $v \sin i$. With knowledge aforesaid, most of the stars can be pushed into the pattern of high Li/high rotation (with the stars in the upper left as rapid rotators seen pole-on) or low Li/slow rotation with the exception of the seven stars in the lower right.

TABLE 8
“MISFITS” WITH HIGH $v \sin i$ BUT LOW $\log N(\text{Li})$

HR	$v \sin i$ (km s^{-1})	$\log N(\text{Li})$	T_e (K)	[Fe/H]	log Age (yr)
4926 ^a	20	≤ 1.57	6370	+0.10	9.35
5533.....	20	1.78	6380	+0.08	9.45
6670.....	30	≤ 1.08	6400	+0.10	9.3
7496.....	21	≤ 1.30	6390	+0.09	9.3
7925.....	30	≤ 1.36	6450	+0.03	ZAMS
7936.....	37	≤ 1.18	6480	+0.04	9.3
8977 ^a	30	≤ 1.41	6620	+0.17	9.2

^a Hyades Moving Group member.

rather low $v \sin i$ values so that line broadening would not reduce the possibility of measuring W_λ .) They are plotted for each star with the value for $\log N(\text{Li})$ in Figure 13. The stars with $\log N(\text{Li}) > 2.4$ are seen at all values of $v \sin i$, but with more between 20 and 40 km s^{-1} (11) than $< 20 \text{ km s}^{-1}$ (6). Similarly, the stars with only upper limits to $\log N(\text{Li}) \leq 1.8$ are found at all $v \sin i$ values but with a greater concentration below $v \sin i < 20 \text{ km s}^{-1}$. High Li and high rotation are expected to go together (e.g., see Soderblom 1982), so it is the low Li points at high $v \sin i$ that are the “misfits.” (The points in the upper left corner could be rapid rotators seen pole-on.) Therefore we have examined the two groups of high $v \sin i$ stars (where “high” $v \sin i$ means 20–40 km s^{-1}): those with high Li [$\log N(\text{Li}) > 2.4$] and those with low Li [$\log N(\text{Li}) \leq 1.8$]. Figure 14 shows the temperature and metallicity distributions for these two subgroups. For the high Li group the temperature and metallicity distributions are similar to the parent group of stars. However, the low-Li, high-rotation “misfits,” listed in Table 8, have metallicities similar to the Hyades (Cayrel *et al.* 1984) and temperatures which fall into the narrow temperature range where the Hyades stars show severe Li depletion (Boesgaard and Tripicco 1986). (In fact two of the stars are in the Hyades Moving Group.) The Hyades stars in this temperature region also show higher rotations (20–50 km s^{-1}) than do their field star counterparts (Kraft 1967). Thus these “misfits” are the Hyades-like stars in

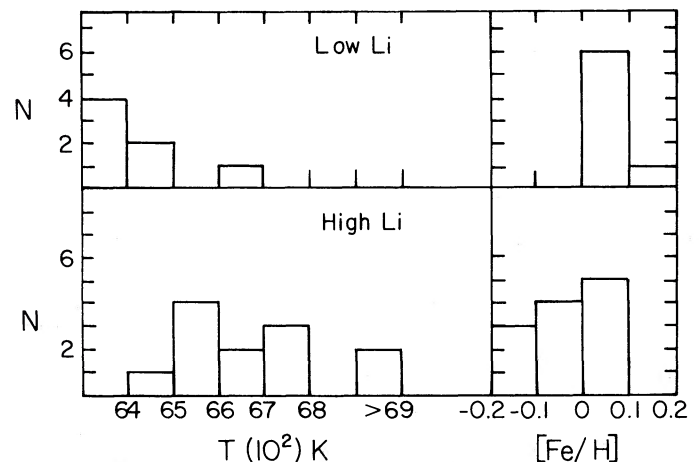


FIG. 14.—The distributions in temperature and metallicity of the seven “misfits” with low Li but high $v \sin i$ from Fig. 13 compared with those distributions for the high Li/high $v \sin i$ stars. The high Li group reflects the distributions of the stars of the total sample while the low Li group looks like the Hyades stars in metallicity and Li in the comparable temperature region.

the field and serve to point out the difficulties of finding coherent patterns in a heterogeneous group of stars.

The general trends discerned from both rotation periods and $v \sin i$ values with Li abundances tend to support the same features found for the field G dwarfs, i.e., stars with higher rotation and greater Li abundance, and those with slow rotation and low Li are the norm.

f) Spectroscopic Binaries

The temperature determinations and equivalent widths and thus the abundances for the double-lined spectroscopic binaries are less certain than for the other F stars. However, some comments should be made. The most surprising case is HR 6985 whose spectrum is shown in Figure 2. According to Abt and Levy (1976) this star probably has a variable radial velocity, but they did not see two spectra. In our three spectra we can clearly see and measure two sets of lines. The Li abundances are different by more than a factor of 15 in the two components. In fact the cooler star ($T_e = 6425$ K) is the one without a detectable Li line; if it were to have the same abundance as the primary, its Li I equivalent width would have to be about 90 mÅ. There is clearly something different, perhaps in the internal structure, between the two stars which leads to this difference in surface Li content. Perhaps it is similar to the cause of the Li deficiencies in the Hyades stars at the temperature of the secondary.

Two of the other pairs show differences in Li content by factors of 5–10. Both components of HR 3579 are depleted, but the hotter star ($T_e = 6580$ K) is more depleted than the cooler ($T_e = 5520$ K) one. The two components of HR 4230 (44 LMi) are within 100 K in temperature of each other at ~ 6800 K, and both are depleted in Li. Although it is not certain, we think that neither component of the RS CVn star, HR 5110, contains Li. The Li contents of two other pairs, HR 6596 (ω Dra) and HR 7000 appear to be comparable to each other and to the initial Li abundance.

V. CONCLUSIONS

With new high-resolution and high signal-to-noise ratio observations of Li in early F stars, we have been able to push Li observations to higher temperature stars and to lower abundance levels. Although early F dwarfs are not expected to be able to reduce their surface Li content by nuclear destruction via mixing below the convection zone, we have found that two-thirds of these stars show substantial Li depletion. We have looked at a number of other observable parameters to try to understand the stellar characteristics which influence the Li destruction.

For the one-third of the sample that do show undepleted Li, we find the initial Li/H abundance relevant to Population I stars, to be $1.02 (\pm 0.34) \times 10^{-9}$ or $\log N(\text{Li}) = 3.01$. This number is similar to (but more accurate than) that found for even younger samples of the galactic disk: the T Tauri stars (Zappala 1972) and the interstellar gas (e.g., Hobbs 1984). These stars are preferentially the hottest stars in our sample, most having $T_e \gtrsim 6600$ K. With the exception of HR 6489, they are all younger than 2×10^9 yr old. In fact this is what would be expected—the hotter, younger F dwarfs would still show their original Li content. The unanticipated aspect is the prevalence and the degree of the depletion in the rest of the early and middle F stars.

In the total sample of 76 (which includes the spectroscopic binaries), 17% show lithium depletion by amounts of 3–10, and

53% by factors of 10–150, i.e., at or below the level of the old halo dwarfs (Spite, Maillard, and Spite 1984). In fact about one-half are down in Li by a factor of 20 or more from $\log N(\text{Li}) = 3.0$, and at least one-quarter are down by more than 50 times [$\log N(\text{Li}) \leq 1.3$].

The F stars that are old according to their kinematic properties—the 10 stars indicated in Table 6—are also rather metal-deficient from our determinations of $[\text{Fe}/\text{H}]$. All of those stars are very Li-depleted with upper limits on $\log N(\text{Li})$ from ≤ 1.38 to ≤ 0.90 , or factors of more than 40 to more than 125. These 10 old-disk stars have apparently been very effective in mixing their original Li content to deeper layers for destruction.

The distributions of Li abundances in the young F stars and in the older F stars are opposite to each other (see Fig. 9). While 62% of the young stars have $\log N(\text{Li}) \geq 2.6$, 64% of the older stars have $\log N(\text{Li}) \leq 1.4$, i.e., they are deficient by factors exceeding 40.

The relationship of Li to age from the results for the F field dwarfs summarized in the last paragraphs can be restated as follows: (a) all but one of the most Li-rich stars are younger than 2×10^9 yr, (b) all of the oldest stars kinematically are very Li-deficient, and (c) there is a dramatic difference in the Li abundance distribution for stars in the two age groups separated at 2×10^9 yr. The Li-age connection for F stars is a broad statistical one, however, since at each age there is a large range in Li abundance. Thus there seem to be other influential parameters involved in determining the Li content.

Metallicity and Li do not seem to be related in F stars with the exception that there are no Li-rich, Fe-poor stars (see Fig. 10). That is, the Li-rich stars all have solar metallicity. This is probably a straightforward reflection of age where older disk stars are poorer in Fe and in Li. The full range of Li values can be found in stars with normal solar Fe and Ca. At values of $[\text{Fe}/\text{H}]$ and $[\text{Ca}/\text{H}]$ from -0.3 to $+0.3$ there is a fairly uniform distribution of $\log N(\text{Li})$ values from <0.9 to 3.2.

Activity, as measured by the Mount Wilson Ca II HK index, is weak in F stars, and only the hint of a trend can be seen in the data available (see Fig. 12). The sense of the trend is that the stars with the strongest HK flux have high Li abundances. It is strongly pulled by the pair of F0 V ZAMS dwarfs, γ Vir N and S, so it may be influenced by age and/or duplicity.

Rotation periods calculated from the activity index were found to be marginally shorter for the Li-rich stars than for the Li-depleted ones. Also the Li-rich stars with high $v \sin i$ values and the Li-poor stars with low $v \sin i$ values (what the relationships found for G dwarfs would predict for F dwarfs) outnumber the opposite pairing (high-Li with low- $v \sin i$ and low-Li with high- $v \sin i$) by two to one. While the high-Li, low- $v \sin i$ stars could be rapid rotators seen pole-on, those with high Li and low $v \sin i$ seem to be a more unusual combination. Such “misfits” have a different distribution in temperature and metallicity than the high-Li/high- $v \sin i$ group and than the parent population. They more nearly resemble the Hyades stars, which have higher $v \sin i$ and $[\text{Fe}/\text{H}]$ values than their field stars counterparts, and which, in the temperature range 6500–6800 K, have been found to be Li-deficient compared to Hyades stars both hotter and cooler (Boesgaard and Tripicco 1986). Some of the field F stars are presumably being depleted in Li by the same mechanism that acts in the Hyades in this temperature range.

The results for the spectroscopic binaries are uncertain, but at least one deserves special notice. The two components of

HR 6985 have temperatures of 6775 and 6425 K and values of $\log N(\text{Li})$ of 3.1 and ≤ 1.9 , respectively. The cooler component must have a different internal structure or mixing mechanism to have destroyed so much Li during the joint history of the pair.

There are several age-related mixing mechanisms that have been proposed to account for Li depletion in solar-type stars. None have specifically predicted the depletions found here for early F stars. Several of these mechanisms which are still plausible but need more detailed calculations to be convincing are the following: meridional circulation and/or convective overshoot, both of which would carry Li atoms to hotter temperatures far below the bottom of the convection zone where they would be destroyed; gravitational settling of Li atoms which would deplete the convection zone from below; and mass loss of the surface layers which would slowly deplete the convection zone from above.

During the course of this work we have had a number of useful discussions about lithium with Drs. P. Bodenheimer, R. and G. Cayrel, G. H. Herbig, and E. Schatzman, and Mr. J. Varsik for which we are very grateful. We are pleased to acknowledge the very professional help at CFHT from the resident astronomers and the telescope operators. We are grateful to Dr. James Heasley and to George Miyashiro for their programming routines and general computing advice during the data reduction. The assistance at Mount Wilson by Dr. D. K. Duncan and Ms. Laura Woodard with the Ca II HK results is gratefully acknowledged. A. M. B. has benefited from an extended stay as a Morrison visitor at Lick Observatory during the final stages of this work and is happy to thank Dr. R. P. Kraft, Director, for the hospitality and for the friendly and stimulating environment there. This work was supported by NSF grant AST 82-16192.

REFERENCES

- Abt, H. A., and Levy, S. J. 1976, *Ap. Suppl.*, **30**, 273.
 Andersen, J., Gustafsson, B., and Lambert, D. L. 1984, *Astr. Ap.*, **136**, 65.
 Baglin, A., Morel, P. J., and Schatzman, E. 1985, *Astr. Ap.*, **149**, 309.
 Blackwell, D. E., Ibbetson, P. A., Petford, A. P., and Willis, R. B. 1976, *M.N.R.A.S.*, **177**, 227.
 Blackwell, D. E., Petford, A. D., Shallis, M. J. and Simmons, G. T. 1982, *M.N.R.A.S.*, **199**, 43.
 Bodenheimer, P. 1965, *Ap. J.*, **142**, 451.
 Boesgaard, A. M. 1976, *Pub. A.S.P.*, **88**, 353.
 Boesgaard, A. M., and Tripicco, M. J. 1985, in preparation.
 ———. 1986, *Ap. J. (Letters)*, **302**, L49.
 Cayrel, R., Cayrel de Strobel, G., Campbell, B., and Dappen, W. 1984, *Ap. J.*, **283**, 205.
 Conti, P. S. 1967, *Ap. J.*, **149**, 629.
 Crawford, D. L. 1975, *A.J.*, **80**, 955.
 ———. 1978, in *Astronomical Papers Dedicated to Bengt Strömberg*, ed. A. Reiz and T. Andersen (Copenhagen: Copenhagen University Observatory), p. 3.
 D'Antona, F., and Mazzitelli, I. 1984, *Astr. Ap.*, **138**, 431.
 Danziger, I. J., and Conti, P. S. 1966, *Ap. J.*, **146**, 392.
 Duncan, D. K. 1981, *Ap. J.*, **248**, 651.
 ———. 1984, *A.J.*, **89**, 515.
 Duncan, D. K., and Jones, B. F. 1983, *Ap. J.*, **271**, 663.
 Eggen, O. J. 1960, *Ap. J.*, **120**, 563.
 ———. 1972, *Ap. J.*, **175**, 787.
 Feast, M. W. 1966, *M.N.R.A.S.*, **134**, 321.
 Gaupp, A., Kuske, P., and Andra, H. J. 1982, *Phys. Rev.*, **A26**, 3551.
 Giannuzzi, M. A. 1979, *Astr. Ap.*, **77**, 214.
 Gilman, P. 1980, in *IAU Colloquium 51, Stellar Turbulence*, ed. D. Gray and J. Linsky (Berlin: Springer-Verlag), p. 19.
 Gurtovenko, E. A., and Kostik, R. I. 1981, *Astr. Ap. Suppl.*, **46**, 239.
 Herbig, G. H. 1965, *Ap. J.*, **141**, 588.
 Herbig, G. H., and Wolff, R. J. 1966, *Ann. d'Ap.*, **29**, 593.
 Hearnshaw, J. B. 1974, *Astr. Ap.*, **34**, 263.
 Hobbs, L. M. 1984, *Ap. J.*, **286**, 252.
 Hoffleit, D. 1982, *Bright Star Catalogue* (4th ed; New Haven: Yale University Observatory).
 Johnson, H. L. 1966, *Ann. Rev. Astr. Ap.*, **4**, 196.
 Kraft, R. P. 1967, *Ap. J.*, **142**, 681.
 Kurucz, R. L. 1979, *Ap. J. Suppl.*, **40**, 1.
 Lambert, D. L., and Luck, R. E. 1978, *M.N.R.A.S.*, **183**, 79.
 Maeder, A. 1976, *Astr. Ap.*, **47**, 389.
 Mazzitelli, I., and Moretti, M. 1980, *Ap. J.*, **235**, 955.
 Moore, C. E., Minnaert, M. G. J. and Houtgast, J. 1966, NBS Monograph 61.
 Nissen, P. E. 1981, *Astr. Ap.*, **97**, 145.
 Noyes, R. W., Hartmann, L. W., Baliunas, S. L., Duncan, D. K., and Vaughan, A. H. 1984, *Ap. J.*, **279**, 763.
 Oblack, E., and Charetan, M. 1980, *Astr. Ap. Suppl.*, **41**, 255.
 Oort, J. 1926, Kapteyn Astr. Lab. Groningen Pub. 40.
 Roman, N. J. 1949, *Ap. J.*, **110**, 205.
 Rutten, R. J., and vander Zalm, E. B. J. 1984, *Astr. Ap. Suppl.*, **55**, 143.
 Skumanich, A. 1972, *Ap. J.*, **171**, 565.
 Soderblom, D. R. 1982, *Ap. J.*, **263**, 239.
 ———. 1985, *Pub. A.S.P.*, **97**, 54.
 Spite, F., and Spite, M. 1982, *Astr. Ap.*, **115**, 357.
 Spite, M., Maillard, J. P., and Spite, F. 1984, *Astr. Ap.*, **141**, 56.
 Strauss, J. M., Blake, J. B., and Schramm, D. H. 1976, *Ap. J.*, **204**, 481.
 Twarog, B. A. 1980, *Ap. J.*, **242**, 242.
 Tomkin, J. R., Lambert, D. L., and Balachandran, S. 1985, *Ap. J.*, **290**, 289.
 van den Heuvel, E. P. J., and Conti, P. S. 1971, *Science*, **171**, 895.
 Vauclair, S., Vauclair, G., Schatzman, E. and Michaud, E. 1978, *Ap. J.*, **223**, 567.
 Walker, G. A. H., Johnson, R., and Yang, S. 1985, *Adv. Electronics Electron Phys.*, **64A**, 213.
 Wallerstein, G., Herbig, G. H., and Conti, P. S. 1965, *Ap. J.*, **141**, 610.
 Wiese, W. L., Smith, M. W. and Miles, B. M. 1969, NSRDS-NBS 22.
 Zappala, R. R. 1972, *Ap. J.*, **172**, 57.

ANN MERCHANT BOESGAARD and MICHAEL J. TRIPICCO: 2680 Woodlawn Drive, University of Hawaii, Institute for Astronomy, Honolulu, HI 96822